Non-Linear Least Squares Optimization for Parametric Identification of DC-DC Converters

G. Rojas-Dueñas, J.-R. Riba, *Member, IEEE* and M. Moreno-Eguilaz

***Abstract*— Switching mode power converters are being extensively applied in different power conversion systems. Parameter identification comprises a set of techniques focused on extracting the relevant parameters of the converters in order to generate accurate discrete simulation models or to design enhanced condition diagnosis schemes. This paper applies a non-invasive optimization approach based on the non-linear least squares algorithm to determine the model parameters of different commercially available DC-DC power converters (buck, boost and buck-boost) from experimental data, including the parameters related to passive, parasitic and control loop elements. The proposed approach is based on a non-invasive on-line acquisition of the input/output voltages and currents under both steady state and transient conditions. The proposed method can also be applied to many other applications requiring precise and efficient parameter identification, including rectifiers, filters, or power supplies among others.**

***Index Terms*— White-box models, switching mode power converters, modelling, parameter identification, optimization.**

I. Introduction

SWITCHING mode power converters (SMPCs) offer interesting features, including high conversion efficiency and compactness [1], [2], which are highly appreciated when designing power conversion systems. They are mostly applied in different applications, including domestic appliances [3], portable electronics, computers and motor drives [4], or in power conversion systems applied to renewable generation [5], among others. Currently, high-tech sectors such as aerospace, naval or automotive are based on complex power systems integrating multiple converters. Such complex power systems often consist of several SMPCs from various suppliers, which usually are reticent to provide detailed information of the internal components [6]. Therefore, habitually, the information available is not sufficient to generate detailed discrete models, although models which are too exhaustive may require unacceptable computational resources [7]. These shortcomings make it difficult to generate accurate dynamic models, especially for the abovementioned high-tech sectors combining several models of SMPCs from different suppliers.

Parameter identification techniques have been applied in different applications, including motor drives [8], power converters [9], load control [10],arc modelling [11], battery and super capacitor systems [12] or transmission lines relaying [13], among others. Parameter identification involves a set of experimental methods focused on obtaining the dynamic behavior of a complex system by applying suitable algorithms. This is a key point, since inaccurate models can have a deep impact on the analysis of power systems [14]. The development of precise parameter identification approaches, which permits accurate and representative replication of the converter behavior, is not a trivial problem, due to the complexity of SMPCs and the wide range of working conditions. Methods based on parameter identification can partly compensate several issues related to different sources of uncertainties to consider during the modelling stage of the SMPCs [15], including the effects of external disturbances, limited load information, component ageing and tolerances or variable ambient conditions among others, which could affect the performance over time of the converter.

Parameter identification approaches are particularly suitable when developing white-box based models, since they require an exhaustive description of the physics laws defining the dynamics of the SMPCs. White-box models usually define the physics of the problem by means of algebraic or differential equations describing its dynamic behavior [16], so precautions must be taken to limit the computational burden [17]. However, other alternatives are possible, such as grey-box and black-box models. Whereas black-box models are based on mathematical models that reproduce or emulate the behavior of the system without describing its behavior from physical equations, grey-box models are not entirely described by physical equations [1].

Parameter identification can also be applied for condition diagnosis purposes in electrical and electronic systems [18], [19], since by analyzing the change in some relevant parameters, the condition of such systems can be diagnosed.

During the modelling and design stages of complex power

This work has been partially supported by the Generalitat de Catalunya under the project 2017SGR0967, the Spanish Ministry of Economy and Competitiveness under the project TRA2016-80472-R and the European Commission through the Clean Sky program, under the project 755332-AEMSIdFit.

G. Rojas-Dueñas is with Electrical Engineering Department, Universitat Politècnica de Catalunya, 08222 Terrassa, Spain (e-mail: gabriel.esteban.rojas@upc.edu).

J.-R. Riba is with Electrical Engineering Department, Universitat Politècnica de Catalunya, 08222 Terrassa, Spain (e-mail: riba@ee.upc.edu).

M. Moreno-Eguilaz is with the Electronics Engineering Department, Universitat Politècnica de Catalunya, 08222 Terrassa, Spain (e-mail: manuel.moreno.eguilaz@upc.edu).

systems involving different SMPCs, design engineers often do not to know most of the parameters in advance [20]. A feasible possibility for parameter identification is to acquire the instantaneous values of the input and output currents and voltages [21] at the input/output terminals of the power converter. This approach is appealing since it is compatible with a non-invasive on-line monitoring of the input/output signals, so there is no need to disconnect or remove the converter from its location when already installed.

This paper proposes to identify the model parameters of different commercial power converters (DC-DC buck, boost and buck-boost converters) by applying an optimization approach. To this end, the non-linear least squares (NLS) algorithm is applied to minimize the error, i.e. the objective function, by estimating step by step the value of the different parameters in the NLS sense, thus minimizing continuously the error function until achieving the optimal solution.

Different strategies are found in the technical bibliography to solve this problem, including off-line and online methods, or methods based on the time- or frequency-domain. In [1] the parameters of a DC-DC converter are identified by solving the differential equations governing the dynamics of the converter, although this approach requires measuring the current in the inductor. In [22] the parameters of a VSC converter are estimated using artificial neural networks, thus requiring a large dataset of training and test signals under different load conditions. In [3] the parameters of a synchronous buck converter are identified by means of a Kalman filter jointly with an adaptive tuning technique, which is applied to improve the tracking performance of the proposed method. In [23] an online identification of the voltage transfer function parameters of a DC-DC converter is carried out by applying a dichotomous coordinate descent method jointly with an infinite impulse response adaptive filter to model the plant. In [24] the frequency response and the transfer function of a buck converter were determined by means of auto-regressive models with exogenous inputs. In [19] the passive components of a boost converter were identified by applying an approach based on wavelet denoising and recursive least squares (RLS). A continuous time model based method is presented in [25], where a polynomial interpolation is applied to calculate the time derivatives involved, together with the least squares algorithm to estimate the passive and parasitic parameters of the converter. The closed loop parameters are estimated in [26] by means of state space models, taking into account the parasitic elements of the DC-DC converter. In [27] the behavior of the converter is approximated by means of a transfer function that is identified using a discrete-time model of the DC-DC converter. Reference [9] reviews different techniques for system and parameter identification of DC-DC power converters. However, all reported methods are invasive, i.e., they require external excitation signals for an effective parameter estimation.

From the literature review it is deduced that most of the papers either identify the converter by means of a transfer function, from which it is not feasible to obtain the real parameters (passive elements and control parameters) of the converter, or only determine some of the parameters. Therefore, there is a need to identify all real parameters of the converter from simple acquisitions of the voltages at the input/output terminals of the converter, since in most cases they are the only accessible sources of information.

This paper proposes a white-box approach for identifying the full set of parameters of buck, boost and buck-boost converters, including the passive, parasitic and control loop elements. Parasitic elements must be considered to model the performances of the DC-DC converter [28]. It is based on acquiring the input/output voltage and current signals at the terminals of the converter, in both steady state (open loop), and transient state (closed loop). It is shown that once the parameters have been identified, the behavior of the converters can be simulated accurately when operating under different conditions by means of a suitable discrete circuit. This paper contributes in several ways. First, it proposes a parameter identification approach which is able to identify the full set of parameters of the converter (between 15 and 18, depending on the converter topology) from experimental data, including the parameters of the passive and parasitic components and those of the PWM control loop. Second, the proposed strategy does not require solving any differential equation governing the behavior of the converter, thus being quite immune to signal noise. Third, the suggested solution allows determining simultaneously all converter parameters from only two measurements performed under steady state and transient conditions. Finally, these measurements are based on acquiring the terminal input/output voltages and currents of the converter, the acquisition procedure being non-invasive and independent of the converter topology.

II. Parameter Identification Based On Nonlinear Least Squares

This section describes the optimization approach based on the nonlinear least squares method (NLS) proposed in this paper to identify the parameters of the DC-DC converters from experimental data. NLS is a technique well suited for identifying parameters of nonlinear systems, i.e. those not satisfying the superposition principle [29], by applying an optimization approach. The NLS algorithm adopted in this paper is based on the trust-region reflective least squares (TRRLS) method, which is a powerful tool to solve constrained bound nonlinear minimization problems [30]. This paper applies the NLS-TRRLS algorithm already incorporated in the Matlab R2019a® package.

In general, the least squares problem consists in finding a vector x that minimizes a sum of squares function e(x) [31],

$$\min_x\left(\|e(x)\|^2\right)=\min_x\left(\sum_{i=1}^{n} e_i^2(x)\right)=\min_x\left(e_1(x)^2+e_2(x)^2+...+e_n(x)^2\right) \quad (1)$$

subjected to linear inequalities $A\cdot x\leq b$ and linear equalities $A_{eq}\cdot x = b_{eq}$, A and A_{eq} being matrixes, b and b_{eq} vectors, $e(x)$ the objective function to be minimized and x a vector, which can have upper and lower bound constraints, ub and lb, respectively, with $lb \leq x \leq ub$. The optimization approach consists of minimizing $e(x)$, which returns scalar values, the inputs of the function being vector arguments x. The objective function is minimized by the identification of a surrounding point that minimizes the value of this function [32].

Under the trust-region optimization approach, supposing the algorithm centered at a point $x \in \Re^n$, to improve the solution it is required to move to a point providing a lower value of *e(x)*. The algorithm is based on approximating *e(x)* by a quadratic function *q(s)*, which reproduces the behavior of *e(x)* in a region N around x, called the trust-region. The objective of the TRRLS method is to calculate *q(s)* using its Taylor series, and to find the trust-region. To this end, the TRRLS computes trial steps s to minimize *q(s)* over *N*, defining the trust-region sub-problem,

$$\min_s \left(q(s),\ s \in N \right) \tag{2}$$

The method calculates *s* step-by-step by minimizing the area of *N*. A successful step accomplishes $e(x+s) < e(x)$, so that the current point *x* is updated by $x + s$ and the trust-region *N* remains for the next step. In case of an unsuccessful step, i.e., $e(x+s) \geq e(x)$, the vector x remains unchanged, and in the next step the trust-region *N* will be reduced. To this end, the interior reflective method generates iterations x_k within the interior of *N* by applying a reflective line search algorithm that ensures convergence at each iteration. The interior of *N* is expressed as int(*N*) and is defined by *ub* and *lb*, Once the scaling transformation is applied to the quadratic function *q(s)*, the standard trust-region sub-problem is defined as [33],

$$\min_s \left(q(s) \right) = \min_s \left(\nabla e(x^k)^T s + \frac{1}{2} s B_k s \right) \text{ with } \left\| D_k^{-1} s \right\| \leq \Delta_k \tag{3}$$

∇ being the partial derivative operator, $\nabla e(x^k)^T$ the gradient of function $e(x)$ at the current point x, $B_k = H_k + D_k^{-1} \mathrm{diag}\left(\nabla f(x^k) \right) J_x(x^k) D_k^{-1}$ a symmetric approximation of the Hessian matrix $H_k = \nabla^2 e(x^k)$, where ∇^2 is the Laplacian operator, $J_x(x^k) = \left(\nabla |v_1|^T \ \nabla |v_2|^T \ldots \nabla |v_n|^T \right)^T$ is the n x n Jacobian matrix and $D_k = \mathrm{diag}\left(\sqrt{|v(x^k)|} \right)$ is a diagonal scaling matrix. The vector $v(x) = \left(v_1(x)\ v_2(x) \ldots v_n(x) \right)^T$ is calculated as,

$v_i = x_i - ub_i$ if $\nabla \left(e(x) \right)_i < 0$ and $ub_i < \infty$

$v_i = x_i - lb_i$ if $\nabla \left(e(x) \right)_i \geq 0$ and $lb_i < \infty$

$v_i = -1$ if $\nabla \left(e(x) \right)_i < 0$ and $ub_i = \infty$

$v_i = +1$ if $\nabla \left(e(x) \right)_i \geq 0$ and $lb_i = -\infty$

Next, by applying a certain x^k, equation (3) is solved to define s^k, so that $x^{k+1} = x^k + \alpha_k s^k$ is obtained, α_k being a step length, which depends on the distance between the boundary of int(*N*) and $x^k + s^k$. Since the region int(*N*) is limited by *lb* and *ub*, the iterations are reflected into int(*N*) when they lie on the boundary, which is known as the reflective line search. Usually, int(*N*) is restricted to a two-dimensional subspace *V*, which is spanned by the vectors *v*. This is done to accelerate the local convergence and enhance the efficiency of the global convergence. After obtaining the subspace *V*, the calculation of eigenvectors and eigenvalues becomes faster and less complex [32].

This paper proposes an objective function as follows,

$$e_i(t) = \left(I_{\text{input}}^{\text{model}}(t) + V_{\text{input}}^{\text{model}}(t) + V_{\text{output}}^{\text{model}}(t) \right)_i - \left(I_{\text{input}}^{\text{experim.}}(t) + V_{\text{input}}^{\text{experim.}}(t) + V_{\text{output}}^{\text{experim.}}(t) \right)_i \tag{4}$$

V and *I* being, respectively, the terminal voltage and current, *n* the number of sample points where $i = 1,2,3,..,n$, $t = i \cdot T$ the time instant considered, and *T* the sampling period of the input/output signals of the DC-DC converter.

To ensure that all signals have the same importance, the input/output currents and voltages are standardized as follows,

$$v^*(t) = (v(t) - v_{mean}) / \sigma_v \tag{5}$$

where $v(t)$ is an input/output voltage or current, v_{mean} the mean value, and σ_v the standard deviation. Since the input/output voltages and currents depend on the converter parameters (passive and parasitic elements and control loop parameters), to obtain the optimal solution it is necessary to restrict the values of the parameters, so that $lb \leq p \leq ub$, p being the model parameters shown in Tables III and IV. Therefore, the NLS-TRRLS algorithm tries to find iteratively the values of the model parameters minimizing the objective function in (1), although the algorithm ends when reaching a predefined tolerance value of the objective function. The lower and upper bounds are chosen based on a priori knowledge of the converter, so that logic upper and lower initial values of the passive elements can be selected.

At each iteration *i*, the values of $\left(I_{\text{input}}^{\text{model}} + V_{\text{input}}^{\text{model}} + V_{\text{output}}^{\text{model}} \right)_i$, which are obtained from the simulation model built in Simulink using the SimPowerSystems™ Toolbox as shown in Fig. 1, change because the NLS-TRRLS algorithm tries new values of the parameters. Therefore, at each iteration the Simulink simulation model is run for several times, since the NLS-TRRLS optimizer calculates a new solution based on the new set of parameters. The ode23tb variable-step continuous solver was used because it is suitable for solving nonlinear stiff problems [34] and in this problem it has faster convergence and higher accuracy than other solvers such as the ode45 and ode15s solvers.

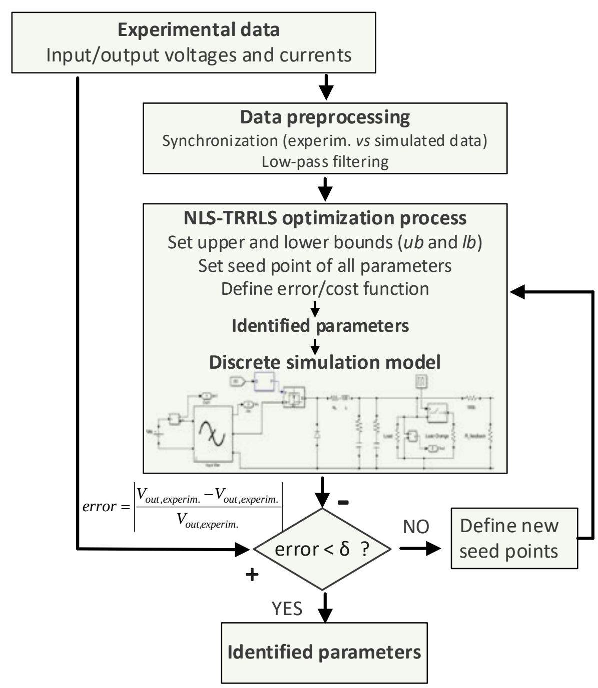

Fig. 1. Flowchart of the proposed parameter identification approach.

Experimental signals exhibit small deviations in the periods, so a preprocessing is required. To this end, one period of the signal is taken and replicated a predefined number of times and next, the signals are filtered by applying a 70 points moving average.

The NLS-TRRLS algorithm estimates the model parameters so that the input/output signals provided by the simulation model are very similar to the experimental ones. The procedure summarized in Fig. 1 is done in two stages. The first one is based on steady state data, whereas the second one is based on transient data, which is obtained by applying a sudden connection of a new load to the output terminals of the converter. From the steady state signals, the passive and parasitic components of the equivalent circuit of the converters are identified, whereas the closed-loop parameters are identified from the transient (load change) signals.

III. The Analyzed DC-DC Converters

This paper identifies the parameters of three non-isolated unidirectional DC-DC converters, namely buck, boost and buck-boost converters, whose topologies are shown in Fig. 2.

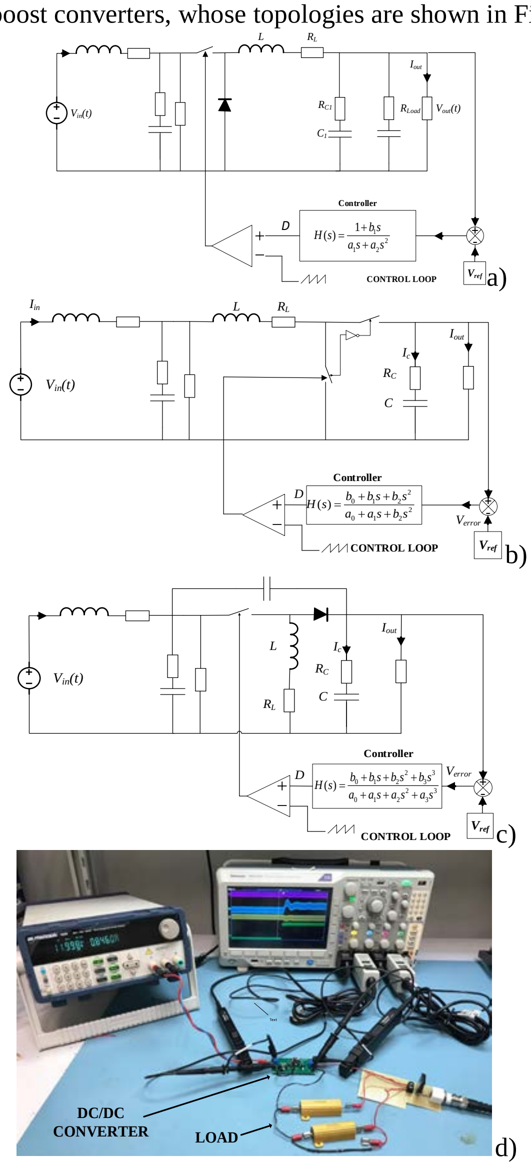

Fig. 2. Analyzed DC-DC converters. a) Buck converter. b) Boost converter. c) Inverting buck-boost converter. d) Photographs of the experimental setup.

Due to the high switching frequency of the power converters analyzed in this paper, some parasitic elements must be considered in the input stage of the discrete simulation models, which are not provided by the manufacturer, although they may affect the performance of the circuit. The parasitic components are the MOSFET on resistance R_S, the ESR of the inductor R_L, the ESR of the output capacitor R_C, and the input capacitor, which is modelled as a capacitance C_{in} in series with the ESR R_{Cin} [35]. The impedance at the output of the voltage source is modelled as a series resistance R_{in} and a series inductance L_{in}, which has an important effect on the shape of the input current. A parallel resistance R_{cc} models the power consumption of the control circuit. According to the manufacturer, the capacitor C_p in the buck-boost converter is used to reduce the output voltage ripple by means of a continuous AC path from the input voltage to the output voltage during the switching states [36]. Table I defines the models and main characteristics of the Texas Instruments DC-DC power converters studied in this work.

The commercial converters described in Table I have been selected because the manufacturer provides most of the values of the parameters, which are summarized in Table II. It is noted that the full set of parameters in Table II are of three types, namely passive, parasitic and control loop elements. Whereas the first two types are identified from steady state data, the last ones are identified from transient data, which is generated under a sudden load change. Parameters with grey shade shown in Table II are recalculated in closed loop since a sensitivity analysis carried out under transient conditions reveled that they influence on the transient response of the converters.

TABLE I
DC-DC Converters Analyzed In This Paper

Converter	Model	Type	Characteristics
Buck	TPS40200EVM-002*	Nonsynchronous	V_{in} = 18-36 V V_{out} = 3.3 V $f_{switching}$ = 200 kHz
Boost	TPS61089EVM-742*	Synchronous	V_{in} = 3.1-5.0 V V_{out} = 9 V $f_{switching}$ = 500 kHz
Buck-boost	TPS5430EVM-342*	Nonsynchronous Inverter mode	V_{in} = 10-15 V V_{out} = -5 V $f_{switching}$ = 500 kHz

*Manufacturer: Texas Instruments, Dallas, TX, USA

IV. Experimental Results

This section describes the experimental results achieved with the three DC-DC converters summarized in Table I. To this end, the input/output voltages and currents were acquired under stationary and transient conditions. Measurements were performed by means of a DC power supply (BK Precision 9205; BK Precision Corporation, Yorba Linda, CA, USA). Input/output voltages and currents were acquired by using a four channel oscilloscope (Tektronix MDO3024 200 MHz 2.5 GS/s; Tektronix, Beaverton, OR, USA), two high-frequency current probes (Tektronix TCP0030A 0.001-20 A 120 MHz; Tektronix, Beaverton, OR, USA) and two high-frequency voltage probes (Tektronix TPP0250 250 MHz; Tektronix, Beaverton, OR, USA). It is important to state that from Fig. 3 to Fig 8, the data of the experimental curves shown were preprocessed by means of a low-pass filter.

To evaluate the accuracy of the proposed method, the results are compared to the ones obtained using the method detailed in [1], which discretizes the differential equations governing the dynamics of the converters, so that the open loop parameters (passive elements) are found. The closed loop (control loop parameters) parameters are estimated by using the duty cycle and the system identification tool of Matlab®.

A. Buck converter

This section presents the identification results from experimental data acquired from the TPS40200EVM-002 buck converter. A step-by-step demo of the procedure is presented, detailing the evolution of the algorithm described in Fig. 1. First, the upper and lower boundaries and the seed point of the parameters are set. These values are defined based in a priori knowledge of the converters, which are shown in Table II.

TABLE II
UPPER AND LOWER BOUNDS FOR THE OPTIMIZATION ALGORITHM

	Minimum	Maximum	Seed point
Inductors	1 nH	1 mH	Random value between the *ub* and *lb*
Capacitors	1 nF	10 mF	
Resistors	0.1 mΩ	10 Ω	
TF coefficients	10^{-12}	10^{-3}	

The objective function is set as the difference between the measured and estimated signals. Then, the process of identifying the open loop parameters is executed. Fig. 3 compares the measured signals and the system simulated using the seed point as the converter parameters

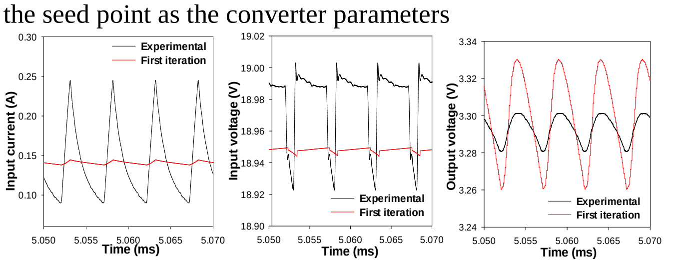

a) b) c)

Fig. 3. Initial point of the first stage of the optimization process. a) Input current. b) Input voltage. c) Output voltage.

The values of the parameters of the first optimization process were: $L = 39.88\mu H$, $C_1 = 17.1\mu F$, $C_2 = 560.4\mu F$, $R_L = 73.1m\Omega$, $R_{C_1} = 59.5m\Omega$, $R_{C_2} = 0.36\Omega$, $R_s = 53m\Omega$ $L_{in} = 0.213\mu H$, $C_{in} = 4.87\mu F$, $R_{C_{in}} = 75m\Omega$, $R_{in} = 0.16\Omega$ and $R_{CC} = 2.57k\Omega$. To estimate the closed loop parameters, the previous values were used as the seed point, and the parameters of the controller (transfer function coefficients) were included in the optimization process. The transient state dataset was used in this stage. Fig. 4 shows the comparison between the measured signal and the starting point of the second stage and the optimization.

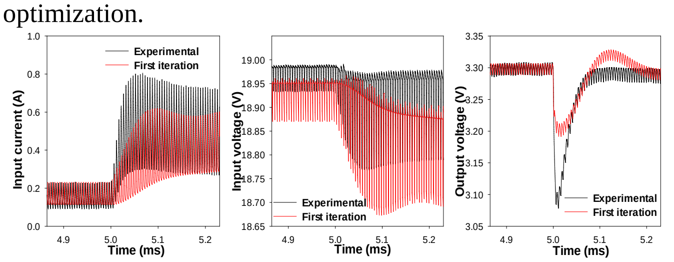

a) b) c)

Fig. 4. Initial point of the second stage of the optimization process. a) Input current. b) Input voltage. c) Output voltage.

Fig. 5 shows the convergence process for the two optimization stages. Compared to the second stage, the first stage, due to the lower number of parameters involved, requires less iterations to achieve the minimum and also the value of the cost function is lower. Finally, once the algorithm reaches the minimum, it finishes and stores the estimated values. The final estimated parameters are shown in the Table III.

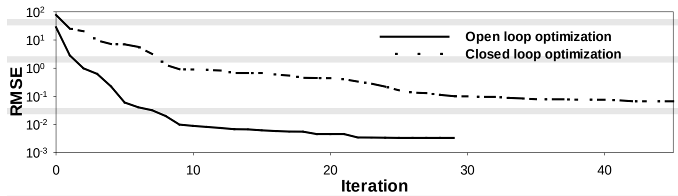

Fig. 5. Boost converter. Convergence process of the two stages of the NLS-TRRLS.

Fig. 6 compares experimental data under steady state conditions (left) and under a sudden load change (right) against the results obtained from the discrete simulation model using the identified parameters (NLS-TRRLS) and the results derived from the analytical equations of the converter [1].

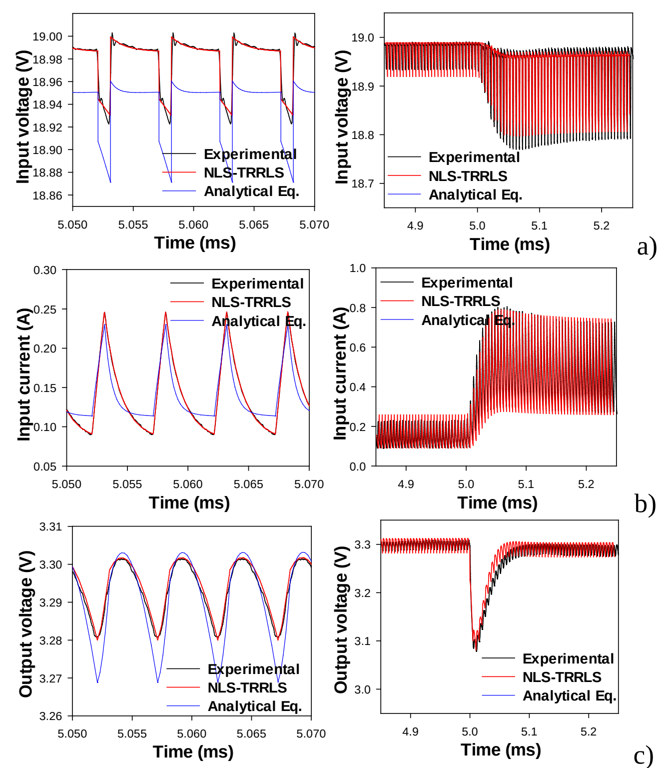

Fig. 6. Buck converter operating under steady state (left) and transient (right) conditions. Experimental versus simulated data using the identified parameters a) Input voltage. b) Input current. c) Output voltage.

The results show a good match between experimental data and simulated results with the identified parameters of the TPS40200EVM-002 buck converter, thus validating the parameter identification approach proposed in this paper. It can be seen that method based on the analytical equations is less accurate in reproducing the transient behavior of the converter.

B. Boost converter

This section presents the identification results from experimental data acquired from the TPS61089EVM-742 synchronous boost converter, following the same procedure as in the case of the buck converter. Two sets of measurements were performed under steady state and transient state (load change). Fig. 7 compares experimental input/output data under steady state conditions (left) and under a sudden load change (right) against the results obtained from the discrete simulation model using the identified parameters (NLS-TRRLS) and the results derived from the analytical equations of the converter [1].

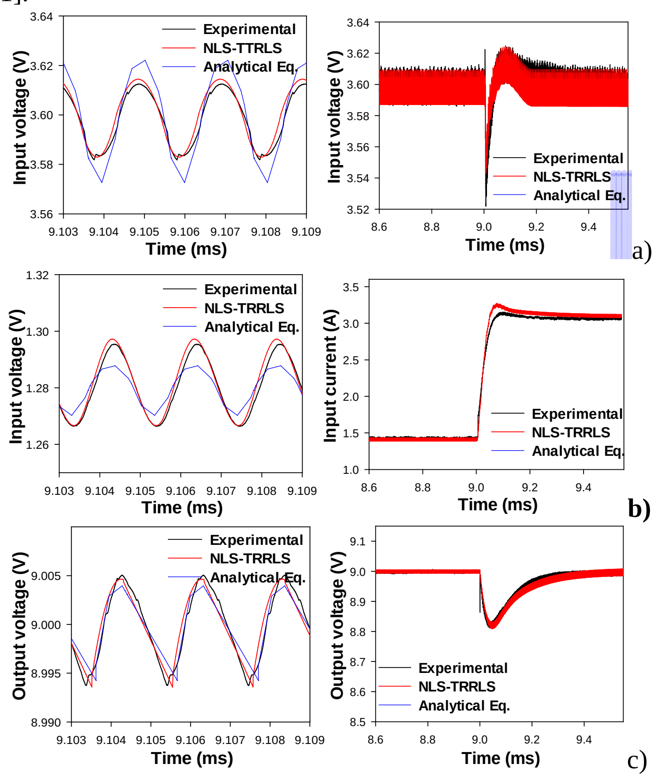

Fig. 7. Boost converter operating under steady state (left) and transient (right) conditions. Experimental versus simulated data using the identified parameters a) Input voltage. b) Input current. c) Output voltage.

Once again, from the results presented in Fig. 7, it can be deduced a close agreement between experimental data and simulated results with the identified parameters of the proposed method (see Table III). The parameter estimation using the analytical equations methods fits well with the measured data in steady state but differs to estimate the transient response.

C. Buck-boost converter

This section summarizes the identification results from experimental data acquired from the TPS5430EVM-342 buck-boost converter.

Fig. 8 compares experimental input/output data under steady state conditions (left) and under a sudden load change (right) against the results obtained from the discrete simulation model with the identified parameters (NLS-TTRLS) and the results derived from the analytical equations of the converter [1]. Figs. 8 show a close similitude between experimental data and simulated results with the identified parameters using the method proposed in this paper. The estimation from the analytical equations is less accurate under a load change.

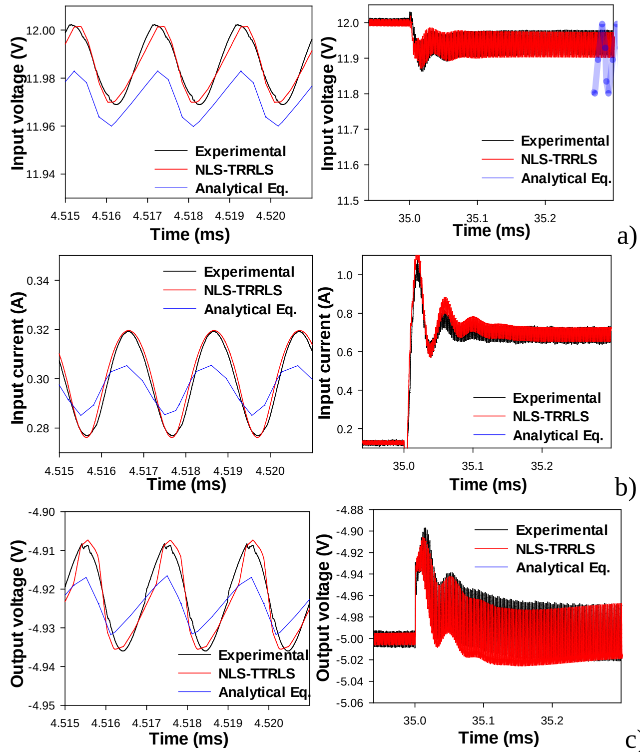

Fig. 8. Buck boost converter operating under steady state conditions (left) and transient (right). Experimental versus simulated data using the identified parameters a) Input voltage. b) Input current. c) Output voltage.

D. Results summary

Tables III and IV compare the parameters provided by the manufacturer of the three analyzed converters, with those identified by means of the approaches presented in this paper. Results summarized in Tables III and IV show a good match between the values of the parameter provided by the manufacturer and those identified by means of the NLS-TRRLS approach. The parameters estimated in open loop show a higher accuracy than those ones estimated in closed loop. This also can be seen in Figs. 6, 7 and 8, where there are slight differences between experimental and estimated data when a load change occurs. One of the main causes is that in closed loop the optimizer considers more parameters. Furthermore, even if the manufacturer provides the transfer function of the control loop, there are different elements of the board that may affect the transient response. Also, the NLS-TRRLS optimization is affected by the noise present in the measurements, even when applying a low-pass filter. Finally, there are elements such as the output impedance of the voltage source and different parasitic components of the DC/DC converters, which were considered in the parameter estimation but not provided by the manufacturer which could affect the identification.

It is noted that the parameters identified using the proposed method show a greater accuracy than the ones identified by solving the analytical equations of the converters. As shown in Figs. 6, 7 and 8, the NLS-TRRLS method has a greater accuracy than the method described in [1], especially under transient conditions. This is because the second method is unable to make an accurate estimation of the controller parameters, as it is shown in Tables III and IV, where the identified values significantly differ from the ones given by the manufacturer. In addition, the analytical equations approach does not consider the input filter of the converter since it uses the current flowing across the inductor.

TABLE III
ACTUAL AND IDENTIFIED PARAMETERS OF THE BUCK AND BOOST CONVERTERS

	Buck				Boost		
	Value	Identified NLS-TRRLS	Identified Analy. Eq.		Value	Identified NLS-TRRLS	Identified Analy. Eq.
$\boldsymbol{L}$	33 µH	35.4 µH	35.2 µH	$\boldsymbol{L}$	1.8 µH	1.7 µH	1.9 µH
$\boldsymbol{C_1}$	20 µF	16.5 µF	16.8 µF	$\boldsymbol{C}$	67 µF	65.6 µF	47.9 µF
$\boldsymbol{C_2}$	440 µF	494.3 µF	490 µF	$\boldsymbol{R_L}$	12.6 mΩ	10.6 mΩ	7.5 mΩ
$\boldsymbol{R_L}$	60 mΩ	73.13 mΩ	55.8 mΩ	$\boldsymbol{R_C}$	0.65 mΩ	0.60 mΩ	1.06 mΩ
$\boldsymbol{R_{C1}}$	65 mΩ	59.5 mΩ	60.9 mΩ	$\boldsymbol{R_{s1}}$	<31 mΩ	38.3 mΩ	10.92 mΩ
$\boldsymbol{R_{C2}}$	300 mΩ	207 mΩ	280 mΩ	$\boldsymbol{R_{s2}}$	-	412.6 mΩ	16.38 mΩ
$\boldsymbol{R_s}$	<40 mΩ	31 mΩ	39.1 mΩ	$\boldsymbol{C_{in}}$	-	40 µF	-
$\boldsymbol{C_{in}}$	100 µF	96.4 µF	-	$\boldsymbol{L_{in}}$	-	0.35 µH	-
$\boldsymbol{L_{in}}$	-	0.40 µH	-	$\boldsymbol{R_{cc}}$	-	2.90 kΩ	-
$\boldsymbol{R_{cc}}$	-	2.57 kΩ	-	$\boldsymbol{R_{Cin}}$	-	5.42 mΩ	-
$\boldsymbol{R_{Cin}}$	-	75 mΩ	-	$\boldsymbol{R_{in}}$	-	0.1 mΩ	-
$\boldsymbol{R_{in}}$	-	0.160 Ω	-	a_0	0	0	0.1
a_0	0	0	-0.01	a_1	$4.7\cdot10^{-9}$	$9\cdot10^{-10}$	$5\cdot10^{-4}$
a_1	$4.7\cdot10^{-4}$	$5.3\cdot10^{-4}$	$1.38\cdot10^{-3}$	a_2	-	$7\cdot10^{-17}$	0
a_2	$1.6\cdot10^{-9}$	$2.8\cdot10^{-9}$	$4.18\cdot10^{-9}$	b_0	1	1	1
b_0	1	1	1	b_1	$8.18\cdot10^{-5}$	$1.42\cdot10^{-4}$	$6.36\cdot10^{-5}$
b_1	$4.7\cdot10^{-4}$	$8.7\cdot10^{-4}$	$7.1\cdot10^{-4}$	b_2	-	$1.05\cdot10^{-9}$	0
b_2	0	0	$1.42\cdot10^{-12}$	-	-	-	-

TABLE IV
ACTUAL AND IDENTIFIED PARAMETERS OF THE BUCK-BOOST CONVERTER

	Buck-Boost		
	Value	Identified NLS-TRRLS	Identified Analy. Eq.
$\boldsymbol{L}$	15 µH	15.41 µH	15.09 µH
$\boldsymbol{C}$	220 µF	292 µF	193.2 µF
$\boldsymbol{R_L}$	41 mΩ	42.26 mΩ	51.1 mΩ
$\boldsymbol{R_C}$	40 mΩ	50.2 mΩ	56.2 mΩ
$\boldsymbol{R_s}$	40 mΩ	46.8 mΩ	28.8 mΩ
$\boldsymbol{C_{in}}$	-	0.354 µF	-
$\boldsymbol{L_{in}}$	-	0.232 µH	-
$\boldsymbol{R_{cc}}$	-	0.27 kΩ	-
$\boldsymbol{R_{Cin}}$	-	2.8 mΩ	-
$\boldsymbol{R_{in}}$	-	48.3 mΩ	-
$\boldsymbol{C_p}$	10 µF	9.31 µF	15.25 µF
a_0	0	0	0
a_1	$7.35\cdot10^{-5}$	$2.78\cdot10^{-5}$	$6.55\cdot10^{-4}$
a_2	$7.0\cdot10^{-10}$	$3.75\cdot10^{-10}$	$5.94\cdot10^{-9}$
a_3	$1.4\cdot10^{-15}$	$1.56\cdot10^{-15}$	$1.00\cdot10^{-15}$
b_0	1	1	1
b_1	$1.4\cdot10^{-4}$	$1.2\cdot10^{-4}$	$3.64\cdot10^{-3}$
b_2	$4.5\cdot10^{-9}$	$4.3\cdot10^{-9}$	$6.16\cdot10^{-8}$
b_3	0	0	0

To measure the accuracy of the estimations, Table V shows the coefficients of determination R^2 between measured and estimated data, which were calculated for the three signals of the three converters. It can be observed that in all cases the values of R^2 are close to 1, thus indicating that the estimation fits the experimental data [37]. The mean value of R^2 for all the cases shown in Table V is 0.9863, while when using the analytical equations of the converter, this value is 0.9449. This indicates that the NLS-TRRLS proposed in this paper is able to reproduce the performance of the DC-DC converters with a higher accuracy than the method proposed in [1].

TABLE V
COEFFICIENT OF DETERMINATION BETWEEN MEASURED AND ESTIMATED DATA

Converter	Operating mode	Coefficient of determination R^2		
		Input voltage	Input current	Output voltage
Buck	Steady State	0.9964	0.9998	0.9981
	Transient	0.9890	0.9951	0.9861
Boost	Steady State	0.9864	0.9902	0.9847
	Transient	0.9785	0.9993	0.9811
Buck-boost	Steady State	0.9810	0.9918	0.9792
	Transient	0.9749	0.9721	0.9705

Table VI summarizes some relevant information about the signals analyzed and the optimization process. The sampling frequency depends on the switching frequency of the converter and whether it works under transient or steady state conditions. It also depends on the instrumentation used.

TABLE VI
SAMPLING FREQUENCY OF THE INPUT/OUTPUT SIGNALS, TIME RANGE, TIME REQUIRED AND NUMBER OF ITERATIONS DURING THE OPTIMIZATION

Converter	Operating mode	Sampling frequency	Identification time*	Iterations	Load
Buck	Steady State	5 GHz	44 minutes	29	5 Ω
	Transient	1 GHz	132 minutes	45	5 + 2.6 Ω
Boost	Steady State	5 GHz	107 minutes	21	18.7 Ω
	Transient	250 MHz	111 minutes	16	18.7 + 18.7 Ω
Buck-boost	Steady State	5 GHz	112 minutes	34	8 Ω
	Transient	250 MHz	368 minutes	54	25 + 4 Ω

The oscilloscope used (Tektronix MDO3024 200 MHz 2.5 GS/s; Tektronix, Beaverton, OR, USA) allows a maximum sampling frequency of 5 GHz and 10^5 points per sample, which is enough to deal with switching frequencies in the range 100-500 kHz. Transient and steady state data must have the same number of data points to be compatible with the algorithms applied. Since transient data requires more periods than steady state data, we had to adapt the sampling frequency to deal with these constraints. Finally, the buck-boost converter requires more identification time, since it has more parameters than the others, thus making the identification process more complex.

V. CONCLUSION

This paper has proposed a parameter identification method for DC-DC power converters based on non-invasive on-line measurements of the voltages and currents at the input/output terminals of the converters. To this end, three types of commercially available DC-DC converters have been analyzed, namely buck, boost and buck-boost converters. The proposed identification method is based on solving an optimization problem by applying the non-linear least squares algorithm, an in particular, the trust-region reflective least squares solver. The results presented in this paper are based on experimental data acquired from the input/output terminals of the converters, considering both steady state and transient operating conditions. Such results prove that it is feasible to identify all model parameters with accuracy, including those related to the passive, parasitic and control loop elements, thus allowing to generate accurate discrete simulation models of the converters. It is worth noting that this method can be applied to identify the parameters of many other devices such as power supplies, rectifiers or filters among others.

FUNDING

This project has received funding from the Clean Sky 2 Joint Undertaking under the European Union's Horizon 2020 research and innovation program under grant agreement No 755332.

Clean Sky 2

This project was funded by the European Union

DISCLAIMER

REFERENCES

[1] J.-R. Riba, M. Moreno-Eguilaz, S. Bogarra, and A. Garcia, "Parameter Identification of DC-DC Converters under Steady-State and Transient Conditions Based on White-Box Models," *Electronics*, vol. 7, p. 393, Dec. 2018.

[2] Qian Shen, L. Ren, C. Gong, and Huizhen Wang, "A unified feature parameter extraction strategy based on system identification for the Buck converter with linear or nonlinear loads," in *IECON 2016 - 42nd Annual Conference of the IEEE Industrial Electronics Society*, 2016, pp. 388–393.

[3] M. Ahmeid *et al.*, "Real-Time Parameter Estimation of DC–DC Converters Using a Self-Tuned Kalman Filter," *IEEE Trans. Power Electron.*, vol. 32, no. 7, pp. 5666–5674, Jul. 2017.

[4] V. Nguyen *et al.*, "Active EMI Reduction Using Chaotic Modulation in a Buck Converter with Relaxed Output LC Filter," *Electronics*, vol. 7, no. 10, p. 254, Oct. 2018.

[5] Y. Zhang *et al.*, "Improved Step Load Response of a Dual-Active-Bridge DC–DC Converter," *Electronics*, vol. 7, no. 9, p. 185, Sep. 2018.

[6] H. Balakrishnan, M. Moreno-Ezuilaz, J.-R. Riba, S. Bogarra, and A. Garcia, "DC-DC Buck Converter Parameter Identification Based on a White-Box Approach," in *2018 IEEE 18th International Power Electronics and Motion Control Conference (PEMC)*, 2018, pp. 242–247.

[7] V. Valdivia, "Behavioral Modeling and Identification of Power Electronics Converters and Subsystems Based on Transient Response," Carlos III (Madrid), 2013.

[8] Z. H. Liu, H. L. Wei, X. H. Li, K. Liu, and Q. C. Zhong, "Global Identification of Electrical and Mechanical Parameters in PMSM Drive Based on Dynamic Self-Learning PSO," *IEEE Trans. Power Electron.*, vol. 33, no. 12, pp. 10858–10871, Dec. 2018.

[9] M. Al-Greer, M. Armstrong, M. Ahmeid, and D. Giaouris, "Advances on system identification techniques for DC-DC switch mode power converter applications," *IEEE Trans. Power Electron.*, vol. 34, no. 7, pp. 6973–6990, Jul. 2019.

[10] S. Gunter *et al.*, "Load Control for the DC Electrical Power Distribution System of the More Electric Aircraft," *IEEE Trans. Power Electron.*, vol. 34, no. 4, pp. 3937–3947, Apr. 2019.

[11] K.-H. Park, H.-Y. Lee, M. Asif, and B.-W. Lee, "Parameter identification of dc black-box arc model using non-linear least squares," *J. Eng.*, vol. 2019, no. 16, pp. 2202–2206, Mar. 2019.

[12] Z. Song, J. Hou, H. F. Hofmann, X. Lin, and J. Sun, "Parameter Identification and Maximum Power Estimation of Battery/Supercapacitor Hybrid Energy Storage System Based on Cramer-Rao Bound Analysis," *IEEE Trans. Power Electron.*, vol. 34, no. 5, pp. 4831–4843, May 2019.

[13] G.Suryanarayana, G.Kesava Rao, S.Sarangi, and P.Raja, "Directional relaying using parameter estimation approach," *Int. J. Electr. Power Energy Syst.*, vol. 107, pp. 597–604, May 2019.

[14] Y. Wang, L. Chao, and Z. Xinran, "Applicability comparison of different algorithms for ambient signal based load model parameter identification," *Int. J. Electr. Power Energy Syst.*, vol. 111, pp. 382–389, Oct. 2019.

[15] M. M. Fawzi Saber Algreer, "Microprocessor Based Signal Processing Techniques for System Identification and Adaptive Control of DC-DC Converters," Newcastle University, 2012.

[16] O. Nelles, *Nonlinear System Identification. From Classical Approaches to Neural Networks and Fuzzy Models.* Springer-Verlag Berlin Heidelberg, 2001.

[17] Petrone, R., Zheng, Z., Hissel, D., Péra, M. C., Pianese, C., Sorrentino, M., … Yousfi-Steiner, "A review on model-based diagnosis methodologies for PEMFCs," *Int. J. Hydrogen Energy*, vol. 38, no. 17, pp. 7077-7091., 2013.

[18] G. Song, J. Luo, S. Gao, X. Wang, and K. Tassawar, "Detection method for single-pole-grounded faulty feeder based on parameter identification in MVDC distribution grids," *Int. J. Electr. Power Energy Syst.*, vol. 97, pp. 85–92, Apr. 2018.

[19] L. Ren and C. Gong, "Modified hybrid model of boost converters for parameter identification of passive components," *IET Power Electron.*, vol. 11, no. 4, pp. 764–771, Apr. 2018.

[20] J. A. Oliver, R. Prieto, V. Romero, and J. A. Cobos, "Behavioural Modelling of DC-DC Converters for Large-Signal Simulation of Distributed Power Systems," *Twenty-First Annu. IEEE Appl. Power Electron. Conf. Expo. 2006. APEC '06.*, no. 1, pp. 1204–1209, 2006.

[21] Y. Wehbe, L. Fan, and Z. Miao, "Least squares based estimation of synchronous generator states and parameters with phasor measurement units," *2012 North Am. Power Symp. NAPS 2012*, 2012.

[22] B. H. Lin, J. T. Tsai, and K. L. Lian, "A Non-Invasive Method for Estimating Circuit and Control Parameters of Voltage Source Converters," *IEEE Trans. Circuits Syst. I Regul. Pap.*, pp. 1–11, Aug. 2019.

[23] M. Algreer, M. Armstrong, and D. Giaouris, "Active Online System Identification of Switch Mode DC–DC Power Converter Based on Efficient Recursive DCD-IIR Adaptive Filter," *IEEE Trans. Power Electron.*, vol. 27, no. 11, pp. 4425–4435, Nov. 2012.

[24] L. Tomesc, B. Betea, and P. Dobra, "Determining the Frequency Response of a DC-DC Converter thru System Identification," *IFAC Proc. Vol.*, vol. 46, no. 6, pp. 149–152, Jan. 2013.

[25] G. M. Buiatti, A. M. R. Amaral, and A. J. M. Cardoso, "An unified method for estimating the parameters of non-isolated DC/DC converters using continuous time models," *Telecommun. Energy Conf. 2007. INTELEC 2007. 29th Int.*, pp. 334–341, 2007.

[26] H. Gietler, C. Unterrieder, A. Berger, R. Priewasser, and M. Lunglmayr, "Low-complexity, high frequency parametric system identification method for switched-mode power converters," *Conf. Proc. - IEEE Appl. Power Electron. Conf. Expo. - APEC*, pp. 2004–2009, 2017.

[27] X. Li, X. Ruan, Q. Jin, M. Sha, and C. K. Tse, "Approximate Discrete-Time Modeling of DC-DC Converters With Consideration of the Effects of Pulse Width Modulation," *IEEE Trans. Power Electron.*, vol. 33, no. 8, pp. 7071–7082, Aug. 2018.

[28] M. Kumar and R. Gupta, "Stability and Sensitivity Analysis of Uniformly Sampled DC-DC Converter with Circuit Parasitics," *IEEE Trans. Circuits Syst. I Regul. Pap.*, vol. 63, no. 11, pp. 2086–2097, Nov. 2016.

[29] S. A. Billings, *Nonlinear system identification : NARMAX methods in the time, frequency, and spatio-temporal domains*, First. Southern Gate, Chichester, West Sussex, PO19 8SQ, United Kingdom: Wiley, 2013.

[30] T. M. Le, B. Fatahi, H. Khabbaz, and W. Sun, "Numerical optimization applying trust-region reflective least squares algorithm with constraints to optimize the non-linear creep parameters of soft soil," *Appl. Math. Model.*, vol. 41, pp. 236–256, Jan. 2017.

[31] Mathworks, "Least-Squares Fitting." Matlab, p. 5, 2019.

[32] M. Ahsan and M. A. Choudhry, "System identification of an airship using trust region reflective least squares algorithm," *Int. J. Control. Autom. Syst.*, vol. 15, no. 3, pp. 1384–1393, Jun. 2017.

[33] T. F. Coleman and Y. Li, "An Interior Trust Region Approach for Nonlinear Minimization Subject to Bounds," *SIAM J. Optim.*, vol. 6, no. 2, pp. 418–445, May 1996.

[34] A. Davoudi, J. Jatskevich, P. L. Chapman, and A. Bidram, “Multi-resolution modeling of power electronics circuits using model-order reduction techniques,” *IEEE Trans. Circuits Syst. I Regul. Pap.*, vol. 60, no. 3, pp. 810–823, 2013.

[35] M. K. Kazimierczuk, *Pulse-Width Modulated DC-DC Power Converters.* Chichester, West Sussex: John Wiley & Sons, Ltd., 2008.

[36] F. De Stasi, “Application Report: Working with inverting buck-boost converters,” Dallas, Texas, 2019.

[37] A. C. Cameron and F. A. G. Windmeijer, “An R-squared measure of goodness of fit for some common nonlinear regression models,” *J. Econom.*, vol. 77, no. 2, pp. 329–342, Apr. 1997.